



Diagnostic performance of ^{18}F -FDG PET and ictal $^{99\text{m}}\text{Tc}$ -HMPAO SPET in pediatric temporal lobe epilepsy: Quantitative analysis by statistical parametric mapping, statistical probabilistic anatomical map, and subtraction ictal SPET

Jong Jin Lee^a, Won Jun Kang^a, Dong Soo Lee^{a,*}, Jae Sung Lee^a,
Hee Hwang^b, Ki Joong Kim^b, Yong-Seung Hwang^b,
June-Key Chung^a, Myung Chul Lee^a

^a Department of Nuclear Medicine, Seoul National University College of Medicine,
28 Yeongeong-dong, Jongno-gu, Seoul 110-744, South Korea

^b Department of Pediatrics, Seoul National University College of Medicine, 28 Yeongeong-dong,
Jongno-gu, Seoul 110-744, South Korea

KEYWORDS

Pediatric;
Temporal lobe
epilepsy;
PET;
SPET;
SPM;
SPAM;
SISCOM

Summary We investigated the diagnostic performance of ^{18}F -FDG PET and ictal $^{99\text{m}}\text{Tc}$ -HMPAO SPET in pediatric temporal lobe epilepsy (TLE). Twenty-one pediatric TLE patients were enrolled in this study. Their diagnoses were confirmed by histology and post-surgical outcome (Engel class I or II). The patients' ages were 18 or younger (15 ± 3 years). Of the 21 patients, 21 patients underwent ^{18}F -FDG PET scan and 15 underwent ictal $^{99\text{m}}\text{Tc}$ -HMPAO SPET. Preoperative PET and/or ictal SPET images were reviewed by simple visual assessment and by statistical parametric mapping (SPM). Asymmetric indices (AI) were calculated using statistical probabilistic anatomical map (SPAM) on ^{18}F -FDG PET. In nine patients who underwent both ictal and interictal SPET, SISCOM (subtraction ictal SPET coregistered to MR template) was performed. PET correctly localized epileptogenic zones in 20 of 21 (95%) by visual assessment. SPM analysis of PET correctly localized epileptogenic zones in 18 of 21 (86%). Ictal SPET correctly localized epileptogenic zones in 12 of 15 (80%) by visual assessment. SPM analysis of ictal SPET correctly localized epileptogenic zones in 12 of 15 (80%). SISCOM correctly localized 8 of 9 (89%), which was equal to that of visual assessment of ictal SPET. The AIs of the temporal lobes by PET were -15 ± 8.4 in the left and 9.9 ± 8.9 in the right TLE (normal control: -2.9 ± 2.8), and correctly localized epileptogenic zones in all cases. As is found in adult TLE, PET and ictal SPET efficiently localized epileptogenic zones in pediatric TLE. SPM analysis of PET or ictal SPET could be used as

* Corresponding author. Tel.: +82 2 760 2501; fax: +82 2 745 7690.
E-mail address: dsl@plaza.snu.ac.kr (D.S. Lee).

an aid to visual assessment. Moreover, SISCOM was equal visual assessment of ictal SPET images in terms of lesion localizations.

© 2005 BEA Trading Ltd. Published by Elsevier Ltd. All rights reserved.

Introduction

In more than 60% of the patients with epilepsy, onset age is less than 20 years.¹ Children have fragile and flexible brain since they are in the developing stage. Neuropsychological damage and brain tissue reduction appear more frequently in childhood-onset temporal lobe epilepsy (TLE) than late onset TLE.² It is also suggested that the plasticity in immature brain may lead to better postoperative recovery of neurologic systems in the children with epilepsy;³ seizure-free outcome has been achieved in 68–78% of children, which is equivalent to that of adult patients.^{4,5}

Surgery in early childhood is therefore recommended for the children with medically intractable temporal lobe seizures.^{5–7} Accurate localization of epileptogenic zones is especially important for the satisfactory prognosis after epilepsy surgery. Indispensable role of functional brain images, such as ¹⁸F-fluorodeoxyglucose (FDG) positron emission tomography (PET) and ^{99m}Tc-hexamethyl-propyleneamine-oxime (HMPAO) ictal perfusion single-photon emission computed tomography (SPET), for localizing the epileptogenic zones is well recognized in adult epilepsy.^{8–11} However, relatively small numbers of studies have been conducted for the pediatric epilepsy. Investigation of the diagnostic performance of the functional brain images for the pediatric epilepsy is therefore encouraged.^{12–14}

Although the reliability of visual assessment of FDG PET and ictal perfusion SPET by the nuclear medicine experts has been established for the localization of epileptogenic zones,¹³ quantitative image analysis methods has also been used as supplementary tools. These techniques, which provide objective and reproducible information for the regional abnormalities in cerebral metabolism and/or perfusion, include: statistical parametric mapping (SPM), statistical probabilistic anatomical map (SPAM), and SISCOM (subtraction ictal SPET coregistered to MRI).^{15–23} SPM, a voxel-based statistical analysis method, is a well known tool to identify the cluster of the voxels in which the difference between a patient (or patients) and normal controls is statistically significant.¹⁶ SPAM is an atlas-based volume of interest (VOI) which is used to obtain regional counts from the spatially normalized individual images into the standardized brain templates.¹⁷ SISCOM is another voxel-based approach and displays an ictal/interictal subtraction

image overlaid on an individual MR image or standard MR template. It is known that SISCOM has superior diagnostic performance to the conventional side-by-side assessment of ictal and interictal images.^{21–23}

The aim of this study was to investigate the diagnostic performance of these approaches using interictal FDG PET and ictal perfusion SPET in pediatric TLE, which is the most common but intractable pediatric epilepsy.^{12–14}

Materials and methods

Patients and controls

Twenty-one children patients with intractable TLE were enrolled in the study. All the subjects had undergone temporal lobectomy and achieved a good surgical outcome (Engel class 1 or 2). Mean postoperative follow-up period was 33 ± 19 months. Postoperative histology excluded the presence of a tumor or any other congenital anomalies. Mean age of the patients was 15 ± 3 years and mean seizure duration was 9.0 ± 4.9 years. Thirteen were boys and eight were girls. Of the 21 patients, 15 patients underwent both PET and ictal SPET. The other six underwent PET alone (Table 1). For the PET analysis, 15 young adult (mean age: 27 ± 7 , M:F = 8:7) volunteers' FDG PET images were used as controls.²⁴ These controls were free of neuropsychological problems, and were receiving no medication known to affect PET study. Informed consents were obtained from these normal control subjects. For the SPET analysis, 17 ^{99m}Tc-HMPAO SPET images of normal healthy children were used as controls (mean age: 10 ± 2.3 , M:F = 11:6). These children were collected retrospectively from the children who had undertaken ^{99m}Tc-HMPAO SPET for evaluation of possible psychiatric abnormalities. They received a neuropsychological assessment and were found to be problem-free.²⁵

PET imaging

An ECAT EXACT 47 Scanner (CTI, Knoxville; spatial resolution $6.2 \text{ mm} \times 6.2 \text{ mm} \times 4.3 \text{ mm}$) was used in this study. ¹⁸F-FDG of 222–370 MBq (adjusted to the body weight) was injected intravenously after at least 6 h of fasting. Patients were in a quiet, dimly lit room with eyes closed for 30 min. Twenty minutes

Table 1 Summary of clinical information.

Patient no.	Diagnosis	Age (years)	Sex	Surgery	Pathology	EEG	MRI	PET	Ictal SPECT	Interictal SPECT	SISCOM	ASI
1	LTLE	18	F	ATL + AH	HS; mild CD	T1	L.HS	LT	LT	LT	LT	-13.5
2	LTLE	12	M	ATL + AH	HS; severe CD	T3, T5	L.HS	LT	LFTP			-9.4
3	LTLE	16	M	ATL + AH	HS; moderate CD	T1	L.HS	LT	LF	N	LT	-9.3
4	LTLE	18	M	ATL + AH	HS; mild CD	LT	L.HS	LT				-8.2
5	LTLE	13	F	ATL + AH	HS; severe CD	T1	L.HS	LT				-8.1
6	LTLE	18	M	ATL + AH	HS; mild CD	T1	L.HS	LT				-6.5
7	LTLE	16	M	ATL + AH	HS; severe CD	T1	L.HS	LT	LT	LT	LT	-5.9
8	LTLE	17	F	ATL + AH	HS; mild CD	T1, T3, F7	L.HS	LT	LT	LT	LT	-5.8
9	LTLE	15	M	ATL + AH	HS	T1 > F7, T3	L.HS	LT				-5.7
10	LTLE	16	M	ATL + NCR + AH	HS; mild CD	T1, T3, F7	L.HS	LT	LT	LT	LT	-5.4
11	LTLE	10	F	ATL + AH	HS; mild CD	T1, T3, F7	L.HS	LT	RFP			-4.6
12	LTLE	18	F	ATL + AH	HS; mild CD	T1 > F7, T3	L.HS	LT	RF			-4.1
13	LTLE	11	F	ATL + AH	HS	T3, T5, T4	L.HS	LT				-0.9
14	RTLE	9	M	ATL + AH	HS; moderate CD	T2	L.HS	N	RT			0.8
15	RTLE	17	M	ATL + AH	HS; mild CD	T2	R.HS	RT	RT	N	N	4.2
16	RTLE	17	M	ATL + AH	HS; moderate CD	T2, T4	R.HS	RT	RT	RT	RT	6.2
17	RTLE	17	F	ATL + AH	HS; mild CD	T2	R.HS	RTO				7.0
18	RTLE	17	M	ATL + AH	HS; mild CD	T2	R.HS	RT	RT	N	RT	10.8
19	RTLE	12	M	ATL + AH	HS; mild CD	T2, T4	R.HS	RT	RTPF	RT	RT	11.9
20	RTLE	6	M	ATL + AH	HS; moderate CD	F8, T4	R.HS	RTF	RFTP			16.6
21	RTLE	16	F	ATL + AH	HS; mild CD	T2	R.HS	RT	RT			17.8

L, left; R, right; TLE, temporal lobe epilepsy; ATL, anterior temporal lobectomy; AH, amygdalohippocampectomy; NCR, neocortical resection; HS, hippocampal sclerosis; CD, cortical dysplasia; F, frontal lobe; T, temporal lobe; P, parietal lobe; O, occipital lobe; N, non-localization; AI, asymmetric index.

after the injection, transmission scan was acquired for 5–7 min using the triple ^{68}Ge rod sources. Afterward, emission scan was acquired for 20 min with 2-dimensional mode. A transmission scan was acquired over 5 min using triple ^{68}Ge rod sources. An emission scan was then acquired over 30 min in the 2-dimensional mode and corrected for photon attenuation using the transmission image. 47 transaxial images were reconstructed using a Shepp-Logan filter (cutoff frequency: 0.35 cycle per pixel). EEG monitoring was not performed during the PET image acquisition but no sign of seizure was detected in all patients.

SPET imaging

Patients were admitted to epilepsy monitoring units. $^{99\text{m}}\text{Tc}$ -HMPAO of 545–1110 MBq (adjusted to body weight) was injected when a seizure started. Injection delay was less than 1 min. The ictal SPET image was acquired within 2 h of injection. To acquire the interictal SPET image, injection of $^{99\text{m}}\text{Tc}$ -HMPAO was repeated during the interictal period more than 3 days after the ictal study.

Both ictal and interictal SPET images were acquired using a triple-head PRISM 3000 SPET camera (Picker International, OH, U.S.A.) with a low energy, high-resolution fan-beam collimator.

One hundred and twenty second images were acquired using the step and shoot method at an interval of 3° with a 128×128 matrix. Transaxial images were reconstructed using filtered back-projection with a Metz filter ($x = 2.5\text{--}3.0$) and realigned to make sagittal and coronal images. Attenuation of photon was corrected using Chang's method (attenuation coefficient = 0.11 cm^{-1}). The slice thickness used was 3.2 mm.

Visual assessment

PET and ictal SPET images were interpreted by two experienced nuclear physicians who were unaware of any clinical information. Coronal, sagittal, and transaxial images were reviewed. Criterion of the correct localization was the significantly increased or decreased intensity in the affected temporal lobe compared to the corresponding regions in the contralateral hemisphere and remote regions of both hemispheres.

SPM analysis

SPM99 (Statistical parametric mapping 99, Institute of Neurology, University of London, U.K.) implemented in Matlab 5.3 (Mathworks Inc., Natick, MA, U.S.A.) was used. The images were spatially normal-

ized to the Montreal Neurological Institute (McGill University, Montreal, Que., Canada) standard templates by linear and non-linear transformation. Count of each voxel was normalized to the whole brain count using proportional scaling method to remove the effects of global intensity. Normalized images were smoothed by convolution with a Gaussian kernel having 16 mm full width at half maximum (FWHM) to increase the signal to noise ratio. Each image of individual patient was compared with images of control group with voxel-by-voxel manner (two-sample *t*-test). The voxels with a *p*-value of less than 0.005 (uncorrected) were considered to be significantly different, and the clusters with more than 100 contiguous voxels (extent threshold, *Ke*) were considered to be of significant size. A *p*-value of less than 0.005 (uncorrected) was adopted according to the previous studies of SPM analysis of epilepsy.^{18,26}

T-value maps of significant voxels were overlaid on the transaxial T1 MR template. Location of epileptogenic zone was assessed in the same manner as in visual analysis. MNI coordinates of the voxel with highest *T*-value in the temporal lobe are summarized in Table 1. Statistical probabilistic anatomical map (SPAM) for the MNI template was used for the anatomical labeling of the coordinates of the voxels. SPAM consists of 98 volumes of interest (VOI) images, and each voxel has the probability from 0 to 1 that belongs to specific region.

Calculation of asymmetry indices

From the spatially- and count-normalized PET images, probability-weighted regional counts were

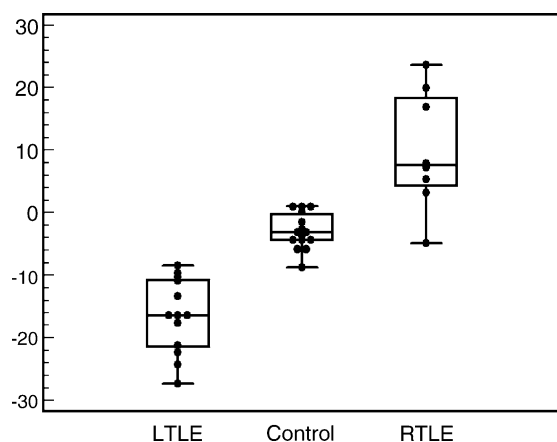


Figure 1 Asymmetric indices (AI) of both temporal lobes. FDG PET was normalized and then multiplied by the SPAM probability. AI indices were calculated using $AI = 200 \times [(counts\ of\ left) - (counts\ of\ right)] / [(counts\ of\ left) + (counts\ of\ right)]$. AIs showed clear distinctions between the groups. The sensitivity of localization by using AI was 100%.

obtained for the 98 VOIs defined by the SPAM.¹⁷ Asymmetry indices (AI) of the regional counts were then calculated by $AI = 200 \times [(counts\ of\ left) - (counts\ of\ right)] / [(counts\ of\ left) + (counts\ of\ right)]$ (Fig. 1).

Subtraction ictal SPET coregistered to MRI (SISCOM)

SISCOM analysis was applied for nine patients who underwent both ictal and interictal SPET¹⁵ scans. Ictal and interictal SPET images were realigned with each other using SPM99. Realigned images were then spatially- and count-normalized and smoothed (FWHM = 16 mm), and the percentage change map between them was obtained. Perfusion changes of more than 20% were regarded as significant and superimposed on a T1 MRI template.¹⁵ The criteria of correct localization were same as in visual assessment.

Localization and statistical analysis

Concordance between the different modalities or between the analysis methods was evaluated using the Cochran *Q*-test (*Q*). Correlation between seizure duration and the *Z*-score was evaluated by using the Spearman rank correlation coefficient (*r_s*). A *p*-value of less than 0.05 was considered significant. SPSS (Version 10.0, Chicago, IL, USA) was used for the statistical analysis.

Results

Diagnostic performance of visual assessment

PET correctly localized 20 of 21 patients (95%) by visual assessment. In two cases, hypometabolic areas extended to ipsilateral frontal or occipital lobes. Ictal SPET correctly localized 12 of 15 patients (80%). In three cases, hyperperfusion areas extended to the ipsilateral frontal and parietal lobes. For patients who underwent both the PET and ictal SPET, PET correctly localized 14 of 15 (93%). No statistical significance was found between the diagnostic performance of PET or SPET in terms of the localization by visual assessment.

Diagnostic performance of SPM analysis

SPM analysis of PET correctly localized 18 of 21 (86%) (Fig. 2). In seven cases of correct localization, clusters of the significant voxels were shown in other brain areas (Table 2). SPM analysis of ictal SPET correctly localized 12 of 15 (80%). There were no

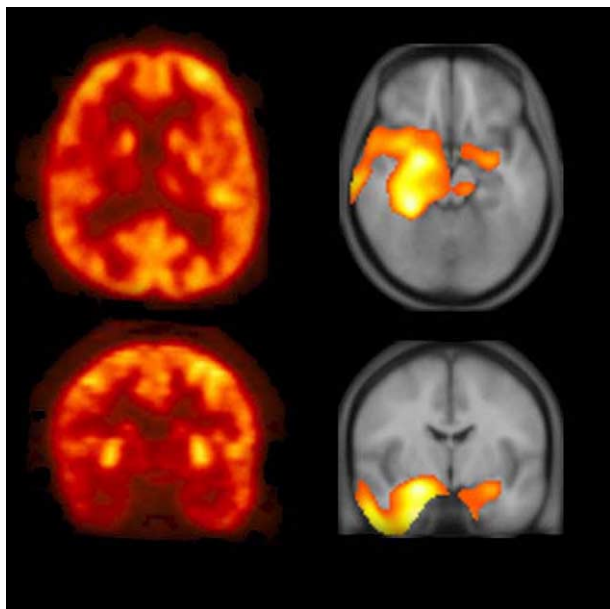


Figure 2 An example of FDG PET and SPM analysis images. SPM analysis was performed at a *p*-value of 0.005, uncorrected. The SPM shows hypometabolic voxels in the right temporal lobe. These images are of one right TLE patient.

clusters of the significant voxels out of the temporal lobe. The SPM cluster extent did not influence the localization sensitivity. No statistical significance was found between the localization sensitivity of visual analysis and SPM for both the PET and SPET.

Asymmetric indices of the temporal lobes in PET

The AI of the whole temporal lobes were -15 ± 8.4 in the left of TLE patients and 9.9 ± 8.9 in the right (normal control: -2.9 ± 2.8). The sensitivity of localization using AI of the temporal lobe was 100%. However, the correlation between seizure duration and the absolute value of Z-score of AI did not show statistical significance.

Diagnostic performance of SISCOM

SISCOM correctly localized 8 of 9 (89%). In these nine cases, visual analysis and SPM analysis of ictal SPET correctly localized 8 of 9 (89%), but not in the same case. No statistically significant difference was

Table 2 SPM results of PET and ictal SPECT.

Patient no.	PET					SPECT				
	Ke	Z	MNI coordinates	Corresponding structure	Another significant cluster	Ke	Z	MNI coordinates	Corresponding structure	
1	49662	6.8	-24, -10, -10	L.parietal lobe		8308	4.74	-62, -6, -12	L.STG	
2	32463	5.72	-32, -40, -14	L.LOTG		57042	5.26	-14, -52, 34	R.parietal lobe	
3	13867	4.67	-42, 10, -38	L.MTG		33204	5.3	-40, 0, -22	L.STG	
4	3961	3.65	-32, -28, -22	L.LOTG	L.inferior frontal gyrus					
5	11824	3.93	-54, 0, -30	L.MTG						
6	1458	3.63	-64, -16, -20	L.MTG	R.thalamus					
7	10364	4.29	-20, -14, -38	L.LOTG		32026	5.47	-40, -2, -22	L.STG	
8	5123	6.34	-32, -40, 66	L.frontal lobe		5052	5.34	-58, -18, -6	L.STG	
9	462	3.15	-32, -30, -22	L.LOTG	L.occipital pole					
10	39616	6.04	-60, -28, -16	L.MTG		8505	5.94	-36, 2, 42	L.frontal lobe	
11	2970	3.77	-56, -4, -26	L.MTG	R.lateral fronto-orbital gyrus	27436	5.07	-40, -2, -22	L.STG	
12	390	3.39	-28, -30, -12	L.HF	L.parietal lobe	35154	5.37	-22, -46, -16	L.LOTG	
13	19127	4.46	-28, -28, -12	L.HF						
14	32634	4.85	14, -22, 8	R.thalamus		1636	4.36	-34, 0, 42	L.frontal lobe	
15	391	3.1	48, 6, -40	R.MTG	R.frontal lobe	23642	5.95	30, 2, -28	R.amygdala	
16	10095	5.02	56, -14, -24	R.MTG		15154	5.83	24, 24, -38	R.MTG	
17	2108	4.35	50, -2, -38	R.MTG	R.middle frontal gyrus					
18	21634	4.74	30, -36, -20	R.LOTG		26582	4.89	44, -12, 0	R.STG	
19	15055	4.86	50, -4, -38	R.MTG		20009	5.85	40, -12, -28	R.STG	
20	49918	6.64	60, -20, -10	R.MTG		9186	4.94	44, -12, 0	R.STG	
21	31796	5.79	58, -14, -26	R.MTG		51409	5.35	44, -10, -6	R.STG	

Ke, extent threshold (number of significant voxels); Z, Z-value of most significant voxel; L, left; R, right; LOTG, lateral occipitotemporal gyrus; MTG, medial temporal gyrus; HF, hippocampal formation; STG, superior temporal gyrus.

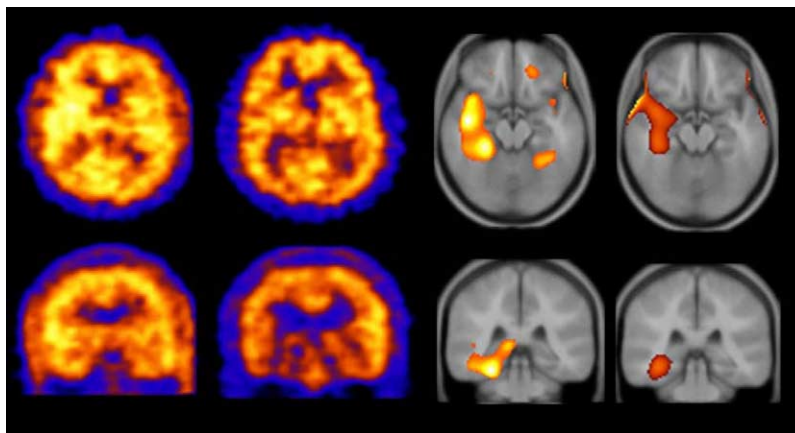


Figure 3 Ictal SPET, interictal SPET, SISCOM, and SPM analysis of ictal SPET images (from left to right). SPM analysis was performed at a p -value of 0.005, uncorrected. These images are of one right TLE patient. SPM analysis of the ictal SPET image shows increased perfusion in right temporal lobe area. SISCOM images show the lesion more clearly than those obtained by SPM analysis of ictal SPET images.

found among the SISCOM, SPM, and visual analysis for ictal SPET in terms of localization. However, SISCOM revealed epileptogenic zones more clearly than the SPM analysis of ictal SPET in most cases (Fig. 3).

Discussion

The localization of epileptogenic zones by PET and ictal SPET is becoming increasingly popular. The introduction of SPM, SPAM, and SISCOM has made nuclear image interpretation more objective. Our study shows that PET and ictal SPET can be successfully used in pediatric TLE.

SPM makes the evaluation of neuroimaging more objective. With certain p -value and cluster size, the voxels with significance are displayed. In this study, SPM analysis was equal to visual analysis in both PET and SPET. SPM is user-independent, reproducible and robust. SPM provides MNI coordinates and we can make good use of them to find the corresponding regions in the brain. Visual analysis tended to be more sensitive than SPM in this study. The stringent p -value may have caused the SPM result less sensitive. However, with looser p -value, the larger extent of abnormality made it difficult to localize the epileptogenic zones. We performed SPM analysis for p -values of 0.01 (uncorrected), 0.005 (uncorrected), 0.001 (uncorrected), 0.05 (corrected), 0.01 (corrected) and found p -value of 0.005 (uncorrected) was relevant with highest sensitivity (data not shown).

As has been found in adult TLE, PET was found to localize epileptogenic zones well in pediatric TLE. Epileptogenic zones typically show hypometabolic areas in interictal FDG PET. However, it has been

suggested by Gaillard et al. that the interictal hypometabolism is related to seizure duration, and therefore, in pediatric epilepsy, especially in younger children, the performance of FDG PET is lower in children than in adults.²⁷ These authors studied children with a mean seizure duration of 1.1 years, whereas the mean seizure duration of our patients, who underwent PET, was 9.0 ± 4.9 years. Our study reveals that, with sufficient seizure duration, one can study a pediatric epilepsy patient by PET to find hypometabolic area.

Ictal SPET was expected to show similar performance in localization of epileptogenic zones to those of SPET in adult TLE. However, much difficulty is also expected whilst performing ictal SPET in children. Little warning, atypical semiology, and poor cooperation combined to make ictal SPET more inaccurate.²⁸ Our study shows that ictal SPET can be performed successfully and provide useful information.

In the SPM analysis of PET, we normalized the patients' PET to the adult template and used the normal young adults' PET images as a control, because normal children's PET images were unavailable. We cannot exclude the possibility of an error due to inherent differences between children and adults. Hermann et al. reported that childhood-onset TLE causes brain volume reduction, especially of white matter.² However, Bentourkia et al. reported that functional maturation is preserved in most parts of brain despite partial epilepsy or anti-epileptic medications, in their brain glucose metabolism study.²⁹ Muzik et al. reported that spatial normalization of the brain of a 6-year-old or more child to an adult template does not result in artifacts in SPM analysis.³⁰ To ensure fidelity, normal control children's PET images should be available.

SPAM produced a certain VOI's count. In the present study, asymmetric indices were calculated using SPAM.¹⁷ A well-known problem of VOI-based analysis is that VOI drawing is operator-dependent and is not robust enough to yield reproducible results.^{13,17} We spatially normalized PET images to the adult template and calculated asymmetric indices using objective population-based MR VOI. Despite the registration of PET to the SPAM template and possible greater partial volume effect in children, our results were very encouraging.

SISCOM was suggested to have better sensitivity of localization than side-by-side ictal and interictal SPET imaging analysis in adult epilepsy patients.^{21,22} However, other authors^{18,31} suggested that SPM analysis of ictal SPET was at least equivalent to SISCOM results. In our study, visual assessment of ictal SPET was equal to SISCOM. Although no statistically significant difference was found in the localizations of SISCOM and the SPM analysis of ictal SPET, SISCOM revealed epileptogenic zones more clearly. This might be because inter-subject variance was larger than within-subject difference. Considering that we luckily had normal control images of children in case of SPET, the results suggested more favor to ictal–interictal difference images of SISCOM. In pediatric epilepsy patients, we suggest that SISCOM is preferable to simple SPM analysis of ictal SPET.

Conclusion

PET and ictal SPET in pediatric TLE were found to have comparable performances in terms of localizing epileptogenic lesions as is the case in adult TLE. SPM could be an objective diagnostic aid in both PET and ictal SPET. AI using SPAM proved to be highly sensitive method of localization, and SISCOM produced results that equaled those obtained by visual assessing ictal SPET images. In summary, the present study shows that SPM, SPAM, and SISCOM can be successfully applied to pediatric TLE.

References

- Morrison G, Duchowny M, Resnick T, Alvarez L, Jayakar P, Prats AR, et al. Epilepsy surgery in childhood. A report of 79 patients. *Pediatr Neurosurg* 1992;18:291–7.
- Hermann B, Seidenberg M, Bell B, Rutecki P, Sheth R, Ruggles K, et al. The neurodevelopmental impact of childhood-onset temporal lobe epilepsy on brain structure and function. *Epilepsia* 2002;43:1062–71.
- Holmes GL. Intractable epilepsy in children. *Epilepsia* 1996;37(Suppl. 3):14–27.
- Wyllie E, Comair YG, Kotagal P, Bulacio J, Bingaman W, Ruggieri P. Seizure outcome after epilepsy surgery in children and adolescents. *Ann Neurol* 1998;44:740–8.
- Duchowny M, Levin B, Jayakar P, Resnick T, Alvarez L, Morrison G, et al. Temporal lobectomy in early childhood. *Epilepsia* 1992;33:298–303.
- Meyer FB, Marsh WR, Laws Jr ER, Sharbrough FW. Temporal lobectomy in children with epilepsy. *J Neurosurg* 1986;64:371–6.
- Dlugos DJ. The early identification of candidates for epilepsy surgery. *Arch Neurol* 2001;58:1543–6.
- Spencer SS. The relative contributions of MRI, SPECT, and PET imaging in epilepsy. *Epilepsia* 1994;35(Suppl. 6):72–89.
- Devous Sr MD, Thisted RA, Morgan GF, Leroy RF, Rowe CC. SPECT brain imaging in epilepsy: a meta-analysis. *J Nucl Med* 1998;39:285–93.
- Won HJ, Chang KH, Cheon JE, Kim HD, Lee DS, Han MH, et al. Comparison of MR imaging with PET and ictal SPECT in 118 patients with intractable epilepsy. *Am J Neuroradiol* 1999;20:593–9.
- Hwang SI, Kim JH, Park SW, Han MH, Yu IK, Lee SH, et al. Comparative analysis of MR imaging, positron emission tomography, and ictal single-photon emission CT in patients with neocortical epilepsy. *Am J Neuroradiol* 2001;22:937–46.
- Grattan-Smith JD, Harvey AS, Desmond PM, Chow CW. Hippocampal sclerosis in children with intractable temporal lobe epilepsy: detection with MR imaging. *Am J Roentgenol* 1993;161:1045–8.
- Lee DS, Lee SK, Lee MC. Functional neuroimaging in epilepsy: FDG PET and ictal SPECT. *J Korean Med Sci* 2001;16:689–96.
- Gaillard WD, White S, Malow B, Flamini R, Weinstein S, Sato S, et al. FDG PET in children and adolescents with partial seizures: role in epilepsy surgery evaluation. *Epilepsy Res* 1995;20:77–84.
- Kim SK, Lee DS, Lee SK, Kim YK, Kang KW, Chung CK, et al. Diagnostic performance of [18F]FDG-PET and ictal [99mTc]-HMPAO SPECT in occipital lobe epilepsy. *Epilepsia* 2001;42:1531–40.
- Van Bogaert P, Massager N, Tugendhaft P, Wikler D, Damhaut P, Levisier M, et al. Statistical parametric mapping of regional glucose metabolism in mesial temporal lobe epilepsy. *Neuroimage* 2000;12:129–38.
- Kang KW, Lee DS, Cho JH, Lee JS, Yeo JS, Lee SK, et al. Quantification of F-18 FDG PET images in temporal lobe epilepsy patients using probabilistic brain atlas. *Neuroimage* 2001;14:1–6.
- Lee JD, Kim HJ, Lee BI, Kim OJ, Jeon TJ, Kim MJ. Evaluation of ictal brain SPET using statistical parametric mapping in temporal lobe epilepsy. *Eur J Nucl Med* 2000;27:1658–65.
- Lee SK, Lee DS, Yeo JS, Lee JS, Kim YK, Jang MJ, et al. FDG-PET images quantified by probabilistic atlas of brain and surgical prognosis of temporal lobe epilepsy. *Epilepsia* 2002;43:1032–8.
- Mazziotta JC, Toga AW, Evans A, Fox P, Lancaster J. A probabilistic atlas of the human brain: theory and rationale for its development The international consortium for brain mapping (ICBM). *Neuroimage* 1995;2:89–101.
- O'Brien TJ, So EL, Mullan BP, Hauser MF, Brinkmann BH, Jack Jr CR et al. Subtraction SPECT co-registered to MRI improves postictal SPECT localization of seizure foci. *Neurology* 1999;52:17–46.
- Kaiboriboon K, Lowe VJ, Chantarujiakong SI, Hogan RE. The usefulness of subtraction ictal SPECT coregistered to MRI in single- and dual-headed SPECT cameras in partial epilepsy. *Epilepsia* 2002;43:408–14.

23. Lee DS, Lee SK, Kim YK, Lee JS, Cheon GJ, Kang KW, et al. Superiority of HMPAO ictal SPECT to ECD ictal SPECT in localizing the epileptogenic zone. *Epilepsia* 2002;**43**:263–9.
24. Lee DS, Lee JS, Kang KW, Jang MJ, Lee SK, Chung JK, et al. Disparity of perfusion and glucose metabolism of epileptogenic zones in temporal lobe epilepsy demonstrated by SPM/SPAM analysis on 15O water PET, [18F]FDG-PET, and [99mTc]-HMPAO SPECT. *Epilepsia* 2001;**42**:1515–22.
25. Kim BN, Lee JS, Shin MS, Cho SC, Lee DS. Regional cerebral perfusion abnormalities in attention deficit/hyperactivity disorder Statistical parametric mapping analysis. *Eur Arch Psychiatry Clin Neurosci* 2002;**252**:219–25.
26. Kim YK, Lee DS, Lee SK, Chung CK, Chung JK, Lee MC. (18)F-FDG PET in localization of frontal lobe epilepsy: comparison of visual and SPM analysis. *J Nucl Med* 2002;**43**:1167–74.
27. Gaillard WD, Kopylev L, Weinstein S, Conry J, Pearl PL, Spanaki MV, et al. Low incidence of abnormal (18)FDG-PET in children with new-onset partial epilepsy: a prospective study. *Neurology* 2002;**58**:717–22.
28. O'Brien TJ, Zupanc ML, Mullan BP, O'Connor MK, Brinkmann BH, Cicora KM, et al. The practical utility of performing perictal SPECT in the evaluation of children with partial epilepsy. *Pediatr Neurol* 1998;**19**:15–22.
29. Bentourkia M, Michel C, Ferriere G, Bol A, Coppens A, Sibomana M, et al. Evolution of brain glucose metabolism with age in epileptic infants, children and adolescents. *Brain Dev* 1998;**20**:524–9.
30. Muzik O, Chugani DC, Juhasz C, Shen C, Chugani HT. Stastical parametric mapping: assessment of application in children. *Neuroimage* 2000;**12**:538–49.
31. Chang DJ, Zupal IG, Gottschalk C, Necochea A, Stokking R, Studholme C, et al. Comparison of statistical parametric mapping and SPECT difference imaging in patients with temporal lobe epilepsy. *Epilepsia* 2002;**43**:68–74.